

ILST Control Algorithm Based Solar Photovoltaic System Using MPPT for Three Phase AC Distribution

T Sudha, P Anand

P.G. Student, Department of Electrical & Electronics Engineering, R.M.K Engineering College, Chennai, Tamilnadu, India¹

Assistant Professor, Department of Electrical & Electronics Engineering, R.M.K Engineering College, Chennai, Tamilnadu, India²

ABSTRACT- This project is new generation technique which is used to develop a double purpose solar photovoltaic system. The first purpose is used to feed the extracted solar energy into the grid and the second purpose is to improve power quality in the three phase AC distribution. The present upgraded system serves the purpose of Maximum Power Point Tracking (MPPT) with fuzzy logic controller. One of the three phase voltage source converter is used for performing all functions of solar photovoltaic system. Additionally an Improved Linear Sinusoidal Tracer (ILST) control algorithm is used to control the Voltage Source Converter (VSC) for feeding solar photovoltaic energy in to the grid and reduce the harmonics. This ILST algorithm is used to provide the switching sequence to the inverter and also balance the grid currents & voltages. The simulation of this system is done by MATLAB.

KEYWORDS- MPPT, three phase inverter, high step- up boost converter, solar photovoltaic and harmonics reduction and grid balancing, ILST.

I.INTRODUCTION

Decreasing reserves of fossil fuels in the world, another major factor working against fossil fuels is the pollution associated with their combustion. Contrastingly, renewable energy sources are known to be much cleaner and produce energy without the harmful effects of pollution unlike their conventional counterparts. Also increasing depletion rates for conventional energy sources have moved world attention on non-conventional energy sources. To meet the load and demand alternate energy source can be needed. Solar power is the conversion of solar energy into a useful form of electrical energy. MPPT System is controlled by Micro controller based unit. Thus reducing the complexity of the system and resulting system has high efficiency and low cost. Ripple correlation control method is used to generate more power by optimization. This method has good response by using optimum input and getting good output. This Photovoltaic system depends on factors such as temperature and solar irradiation results in high cost and low efficiency. To overcome this P&O (Perturbation and Observation) method is used. This experiment results in finding maximum power points under rapid irradiation variations. The main objective is reducing the maximum cost. It will be sustaining all environmental conditions and it utilizes Pulse Width Modulation technique to regulate the output power. This system is designed by MATLAB Simulink modal. Grid connected PV system using three MPPT controls is simulated and compared. The simulation results have verified the tracking efficiency and speed of proposed MPPT. The MPPT algorithm tracks current and voltage in changing the environment. An improved linear sinusoidal tracer (ILST)-based control technique for fundamental extraction is proposed and based on that, an adaptive linear sinusoidal tracer (ALST)-based system for improvement in power quality. However, in the presented work an improvement in ALST algorithm is proposed, along with feature of real power injection into the grid. A comparison of proposed and ALST algorithm is presented in Section III. The proposed SPV system extracts maximum power from PV array and feeds that power into the three-phase distribution system. An incremental conductance MPPT algorithm is used to extract power from the PV string. In this paper, a grid interfaced solar PV energy conversion system is proposed which performs the functions of harmonics mitigation, power factor correction, and grid currents balancing. A grid current

balancing is an important aspect as it allows effective and efficient utilization of an existing distribution system. The control algorithm used for such grid interfaced system is based on ILST algorithm. The unique features of ILST control algorithm are simple control, fast convergence, and its internal parameters have physical significance. Although some researchers have suggested grid interfaced single-stage three phase system as active power filter on cloudy days and solar energy conversion system on sunny days but none of them have shown the implementation of both the features at the same time with grid currents balancing feature in three-phase system. The simulation of the complete system is carried out in MATLAB/Simulink environment. Detailed results for steady state and dynamic conditions are presented to demonstrate its all features. The system response satisfies IEEE standards.

ILPROPOSED SYSTEM

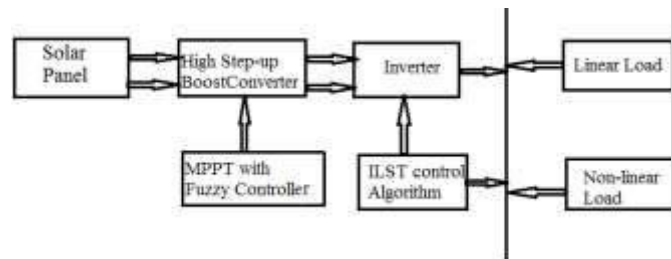


Fig.1. Configuration of SPV energy conversion system.

The energy obtained from the solar panel is given to the High step-up Boost Converter and the MPPT – Fuzzy Optimization Algorithm is implemented in High step- up Boost Converter to trap the maximum power and maintain the voltage at the output. The regulated output from the converter is given to the Voltage Source Converter (VSC) which is controlled through Improved Linear Sinusoidal Tracer (ILTS) algorithm and the output of VSC is connected to the grid and used for non linear compensation.

III. SYSTEM CONFIGURATION

The SPV conversion process consists of PV cells, high step-up boost converter, three phase inverter, MPPT circuit and ILST algorithm, and a ripple filter. A PV string consists of series parallel combination of small photovoltaic modules to match the required power rating. The SPV energy conversion system is interfaced to a three-phase distribution system. Connected loads may be linear or nonlinear in nature which may be compensated by VSC of SPV system. A floating dc link structure is used unlike two stage topology with fixed dc link voltage. The VSC performs the functions of MPPT, harmonics elimination, balancing of grid currents, and power factor correction at the same time with the proper control. The interfacing inductors and ripple filter are used to filter switching harmonics. Therefore MPPT techniques are needed to maintain the PV array's operating at its MPP [comparison]. Many MPPT techniques have been proposed in the literature; example are the Perturb and Observe (P&O) methods, Incremental Conductance (IC) methods, Fuzzy Logic Method. In this paper two most popular of MPPT technique (Perturb and Observe (P&O) methods and Incremental Conductance methods).

IV. MODELLING OF PHOTOVOLTAIC PANEL

A PV array consists of several photovoltaic cells in series and parallel connections. Series connections are responsible for increasing the voltage of the module whereas the parallel connection is responsible for increasing the current in the array. Typically a solar cell can be modeled by a current source and an inverted diode connected in parallel to it. It has its own series and parallel resistance. Series resistance is due to hindrance in the path of flow of electrons from N to P junction and parallel resistance is due to the leakage current.

In this model we consider a current source (I) along with a diode and series resistance (Rs). The shunt resistance (RSH) in parallel is very high, has a negligible effect and can be neglected.

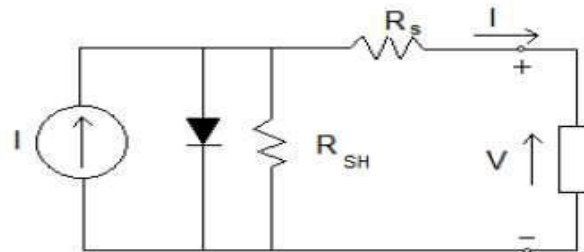


Fig.2. Single diode model of a Photovoltaic cell

The output current from the photovoltaic array is

$$I = I_{sc} - I_d \quad (1)$$

$$I_d = I_o (e^{qV_d/kT} - 1) \quad (2)$$

Where,

I_o is the reverse saturation current of the diode, q is the electron charge,

V_d is the voltage across the diode,

k is Boltzmann constant (1.38×10^{-19} J/K) and T is the junction temperature in Kelvin (K).

From above eqns.

$$I = I_{sc} - I_o (e^{qV_d/kT} - 1) \quad (3)$$

Using suitable approximations,

$$I = I_{sc} - I_o (e^{q(V+IR_s)/nkT} - 1) \quad (4)$$

Where,

I is the photovoltaic cell current, V is the PV cell voltage,

T is the temperature (in Kelvin) and n is the diode ideality factor.

In order to model the solar panel accurately we can use two diodes model but in our project our scope of study is limited to the single diode model. Also, the shunt resistance is very high and can be neglected during the course of our study

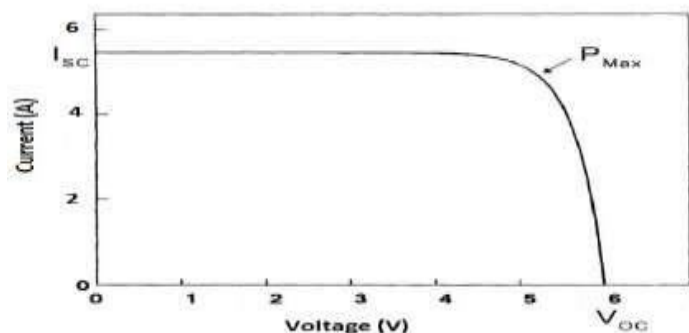


Fig.3. I-V characteristics of a solar panel

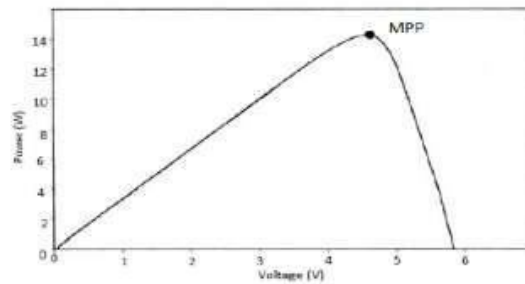


Fig.4. P-V characteristics of a solar panel

The I-V characteristics of a typical solar cell are as shown in the Fig.3. When the voltage and the current characteristics are multiplied we get the P-V characteristics as shown in Fig.4. The point indicated as MPP is the point at which the panel output power is Maximum

SIMULATION CIRCUIT OF SPV:

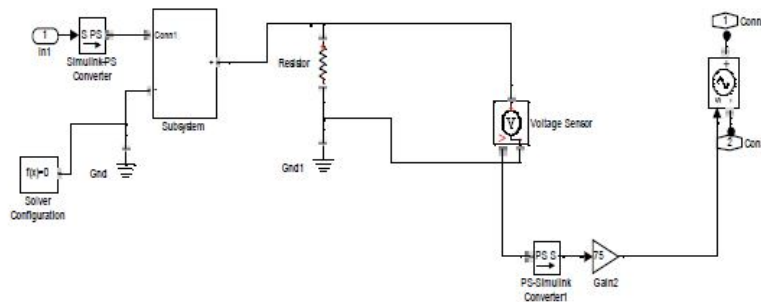


Fig.5. Photovoltaic panel simulation circuit diagram

The Fig.6 & Fig.7 represents the waveform of the Solar Panel Output Voltage and current. In the below graph the X-axis

represents the time period and Y-axis represents the amplitude of the Solar Photovoltaic Voltage and amplitude of current. From the waveform we can observe the output voltage range is 42V and output current range is 6.8A.

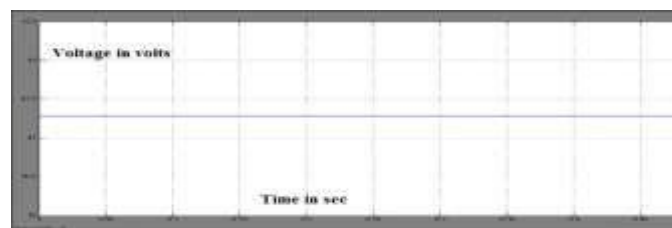


Fig.6. Solar panel output voltage waveform



Fig.7. Solar panel output current waveform

TABLE I Simulation results of SPV

Quantity	Value
Input voltage	12v
Output Voltage	42v
Output Current	6.8v
Output Power	285.6w

Table 1 simulation results of solar panel

V.HIGH STEP –UP BOOST CONVERTER

A high step-up dc/dc converter is used to convert low voltage into high voltage. The converter is characterized by low input current ripple and low conduction losses, which increases the lifetime of renewable energy sources and makes it suitable for high-power applications. The converter achieves the high step-up gain that renewable energy systems require. Due to the lossless passive clamp performance, leakage energy is recycled to the output terminal. Hence, large voltage spikes across the main switches are alleviated, and the efficiency is improved. Low cost and high efficiency are achieved by employment of the low-voltage-rated power switch with low RDS (ON); also, the voltage stresses on main switches and diodes are substantially lower than output voltage. [2]

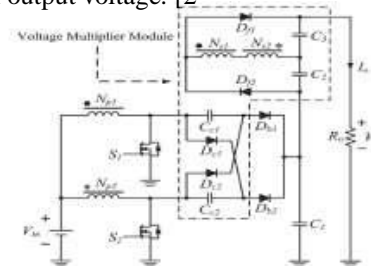


Fig.8. Functional Block Diagram of high step-up boost converter

Where,

Lm1 & Lm2 = magnetizing inductors.

Lk1 & Lk2 = leakage inductors.

Ls = series leakage inductors in the secondary side.

S1 & S2= power switches.

International Journal of Innovative Research in Science, Engineering and Technology

An ISO 3297: 2007 Certified Organization

Volume 4, Special Issue 5, April 2015

International Conference On Emerging Trends in Engineering and Technology (ICETET'15)

On 13th & 14th March 2015

Organized by

Pandian Saraswathi Yadav Engineering College, Arasanoor, Sivagangai, Tamilnadu, India

Cc1 & Cc2 = switched capacitors.

C1, C2&C3 = output capacitors.

Dc1 & Dc2 = clamp diodes.

Db1 & Db2 = output diodes for boost operation with switched capacitors.

Df1 & Df2 = output diodes for fly back-forward Operation

N = turns ratio (Ns/Np)

Output waveform of high step-up boost converter:

The Fig.18 & Fig.19 represents the waveform of the high step-up boost converter output voltage. In the below graph the x-axis represents the time period and y-axis represents the amplitude of the boost converter output voltage and output current. From the waveform we can observe the output voltage range is 420V.

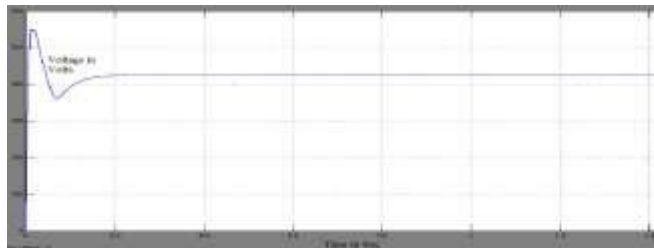


Fig.9. Output voltage waveform

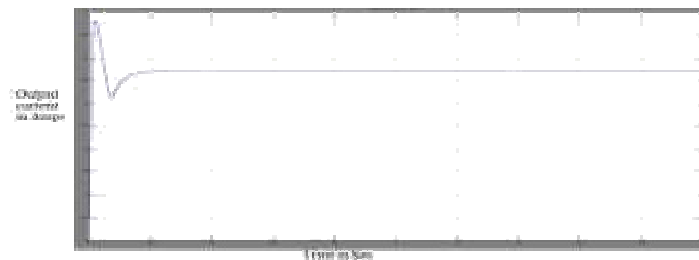


Fig.10. Output current waveform

TABLE.II. Simulation results of high stepup boost converter

Quantity	Value
Input Voltage	42 V
Output voltage	420V
Output current	3.7A
Frequency	10 KHz
Duty cycle	(0.1<D<0.9)

VI. THREE PHASE INVERTER MODELLING

Inverter is a device used to convert the DC current to AC current. Normally inverter works on two modes of operation according to the number of switches conduct per each cycle. There are two modes are available, 180 degree and 120 degree mode. The output of the three phase inverter is a square wave hence the filter circuit is used to convert it to a pure sine wave.

180° Conduction Mode Diagram:

Three switches are in ON state at a time

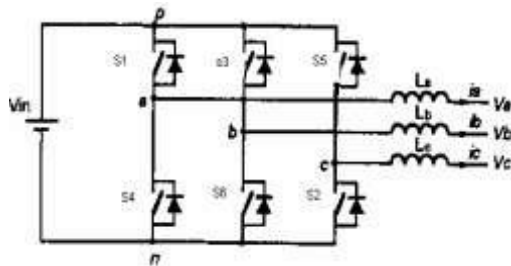


Fig.11. Circuit diagram of 180° conduction mode

Three phase Voltages for 180°Conduction:

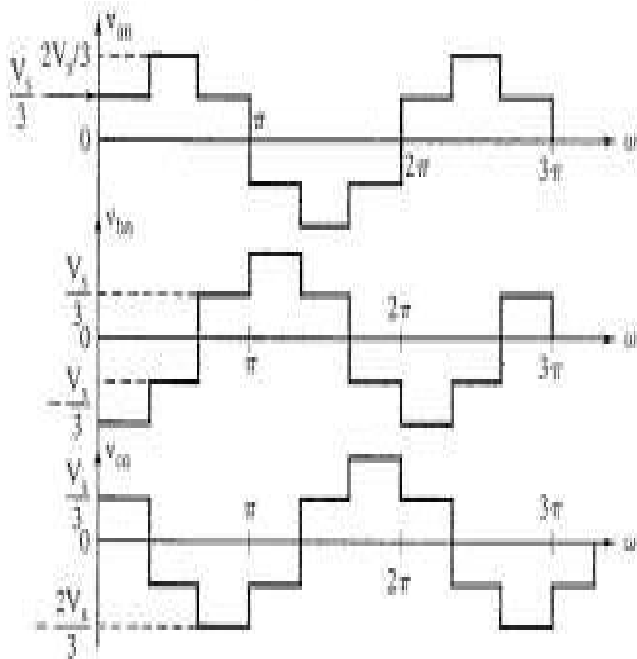


Fig.12. Waveform of 180° conduction mode

International Journal of Innovative Research in Science, Engineering and Technology

An ISO 3297: 2007 Certified Organization

Volume 4, Special Issue 5, April 2015

International Conference On Emerging Trends in Engineering and Technology (ICETET'15)

On 13th & 14th March 2015

Organized by

Pandian Saraswathi Yadav Engineering College, Arasanoor, Sivagangai, Tamilnadu, India

TABLE.III. Switching Sequence Summary

State	Static No.	Switch States	Vab	Vbc	Vbc
s1,s2 and s6 are on and s4,s5,s3 are off	1	100	Vs	0	-Vs
s2,s3,s4 on and s6,s5, s1 off	2	110	0	Vs	-Vs
s3,s4,s2 on and s1,s5,s6 off	3	010	-Vs	Vs	0
s4,s3,s5 on and s1,s2,s6 off	4	011	-Vs	0	Vs
s5,s6,s4 on and s1,s2,s3 off	5	001	0	-Vs	Vs
s6,s1,s5 on and s2,s3,s4 off	6	101	Vs	-Vs	0
s1,s3,s5 on and s2,s4,s6 off	7	111	0	0	0
s4,s6,s2 on and s1,s3,s5 off	8	000	0	0	0

Output Waveform of three phase inverter:

The Fig.13 represents the waveform of the three phase inverter output voltage. In the below graph the x-axis represents the time period and y-axis represents the amplitude of the three phase inverter output voltage. From the waveform we can observe the output voltage range is 420V

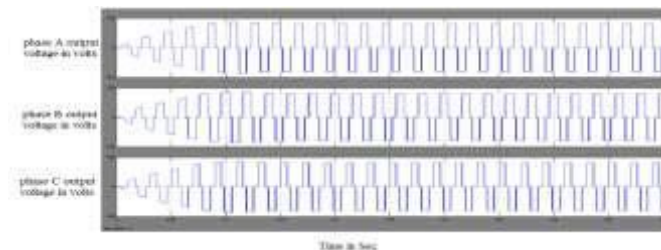


Fig.13 Three phase inverter output voltage waveform

VII. ILST MODELLING

ILST is the Linear Sinusoidal Tracer algorithm. It is mainly used to give input switching sequence to the inverter based on the output voltage and output current from that same inverter and also used to control the voltage source converter. The sensed voltages of solar panel are first passed through band pass filter to eliminate switching noise and any other harmonics present. Simple mathematical operations are applied to convert line voltages to phase voltages, output of three phase voltages are V_{sa} , V_{sb} and V_{sc} . An amplitude transformation is applied to estimate amplitude of phase voltages. Finally an ILST algorithm is used to extract fundamental and reference current.

Procedure

The amplitude of the phase voltage is estimated as,

$$V_p = \sqrt{\frac{2(V_{sa}^2 + V_{sb}^2 + V_{sc}^2)}{3}} \dots\dots\dots (5)$$

Using estimated peak voltage, in-phase unit templates are estimated as

$$x_{ap} = \frac{V_{sa}}{V_p}; x_{bp} = \frac{V_{sb}}{V_p}; x_{cp} = \frac{V_{sc}}{V_p} \dots\dots\dots (6)$$

From in-phase unit templates, quadrature (90° shifted) unit templates are derived as

$$\begin{aligned} x_{ap} &= -x_{bp}/\sqrt{3} + x_{cp}/\sqrt{3} \\ x_{bp} &= \sqrt{3} x_{ap}/2 + (x_{bp} - x_{cp})/2 \sqrt{3} \\ x_{cp} &= -\sqrt{3} x_{ap}/2 + (x_{bp} - x_{cp})/2 \sqrt{3} \dots\dots\dots (7) \end{aligned}$$

ILST Circuit Diagram

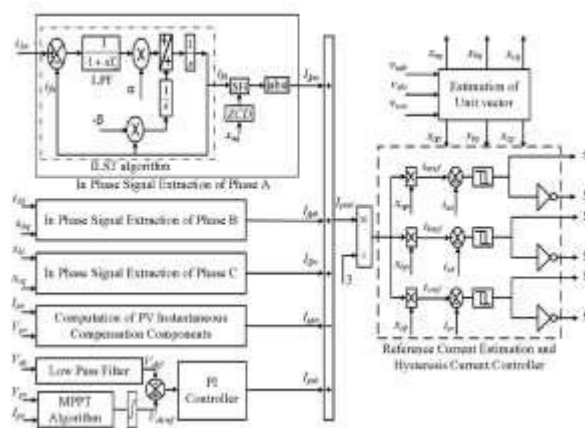


Fig.14. ILST block diagram

ILST Waveform:

The Fig.15 represents the waveform of the fundamental current. In the below graph the x-axis represents the time period and y-axis represents the amplitude of the fundamental current. From the waveform we can observe the output current range is 2.4A

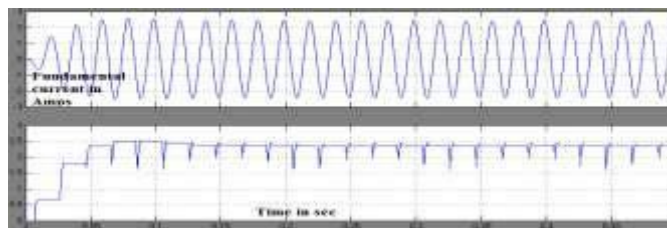


Fig.15 ILST fundamental current waveform

The Fig.16 represents the waveform of the reference current. In the below graph the x-axis represents the time period and y-axis represents the amplitude of the reference current. From the waveform we can observe the output current range is 0.45A

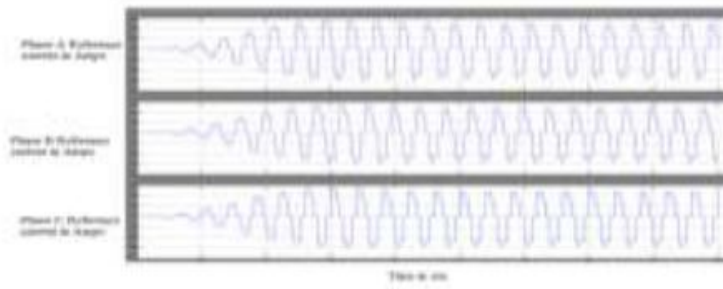


Fig.16 ILST reference current waveform

VIII. FUZZY LOGIC MODELLING

Fuzzy logic controllers are useful when the system dynamics contains non-linearities and membership functions are suitable for the input and output, which gives more sensitivity. Fuzzy logic is a form of many-valued logic; it deals with reasoning that is approximate rather than fixed and exact. In contrast with traditional logic theory, where binary sets have two-valued logic: true or false, fuzzy logic variables may have a truth value that ranges in degree between 0 and 1. Fuzzy logic has been extended to handle the concept of partial truth, where the truth value may range between completely true and completely false.

Structure of Fuzzy logic system:

A fuzzy logic system (FLS) can be defined as the nonlinear mapping of an input data set to a scalar output data. A FLS consists of four main parts: fuzzifier, rules, inference engine, and defuzzifier. These components and the General architecture of a FLS are shown in Fig.17

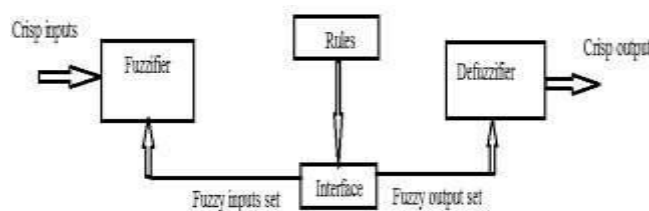


Fig.17 General Architecture of fuzzy logic system

The process of fuzzy logic is explained in Algorithm 1: Firstly, a crisp set of input data are collected and converted into a fuzzy set using fuzzy linguistic variables and membership functions. This step is known as fuzzification. And then, an inference is made based on a set of rules. Finally, the resulting fuzzy output is mapped to a crisp output using the membership functions, in the defuzzification step.

Linguistic variables:

While variables in mathematics usually take numerical values, in fuzzy logic applications, the non-numeric linguistic variables are often used to facilitate the expression of rules and facts. A linguistic variable such as age may have a value such as young or its antonym old. However, the great utility of linguistic variables is that they can be modified via linguistic hedges applied to primary terms. The linguistic hedges can be associated with certain functions.

Example

Fuzzy set theory defines fuzzy operators on fuzzy sets. The problem in applying this is that the appropriate fuzzy

International Journal of Innovative Research in Science, Engineering and Technology

An ISO 3297: 2007 Certified Organization

Volume 4, Special Issue 5, April 2015

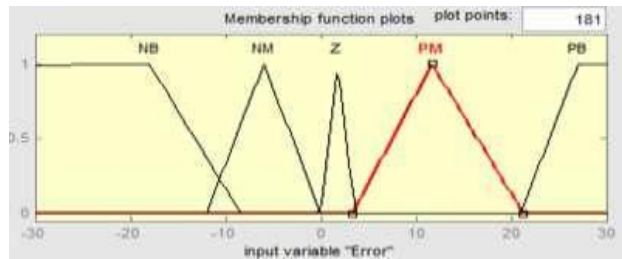
International Conference On Emerging Trends in Engineering and Technology (ICETET'15)

On 13th & 14th March 2015

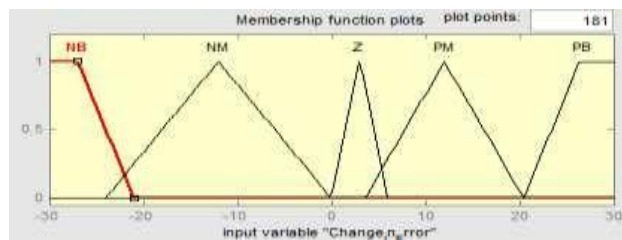
Organized by

Pandian Saraswathi Yadav Engineering College, Arasanoor, Sivagangai, Tamilnadu, India

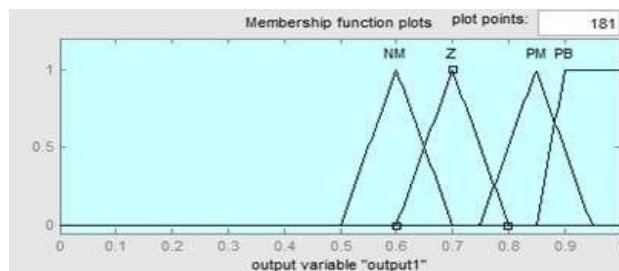
operator may not be known. For this reason, fuzzy logic usually uses IF-THEN rules, or constructs that are equivalent, such as fuzzy associative matrices.



Membership functions for error input



Membership functions for change in error



Membership functions for output

TABLE.III. Rules for Fuzzy Controller

Error CE	NB	NM	Z	PM	PB
NB	PB	NM	PB	NM	PNN
NM	NM	Z	PM	PB	PNN
Z	Z	PNN	PM	PB	PB
PM	PB	PM	PB	PM	PNN
PB	NM	Z	PM	PB	NM

Maximum Power Point Tracking Modelling:

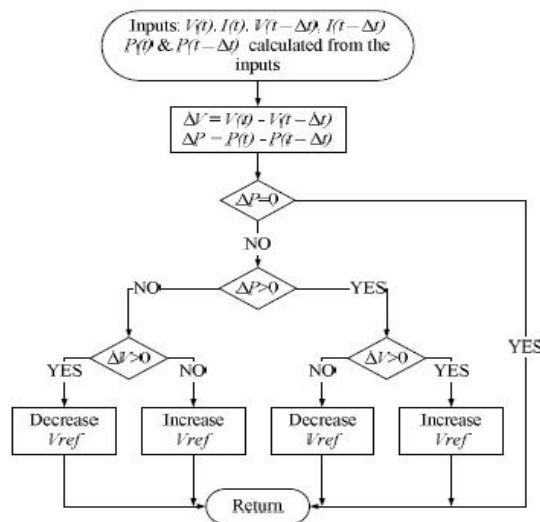


Fig.18. Flow chart of P&O algorithm

The Fig.16 represents the waveform of the duty cycle. From the waveform we can observe the duty cycle value is 0.83



Fig.16 Duty cycle Vs time waveform

SIMULATION OF PROPOSED MODELLING:

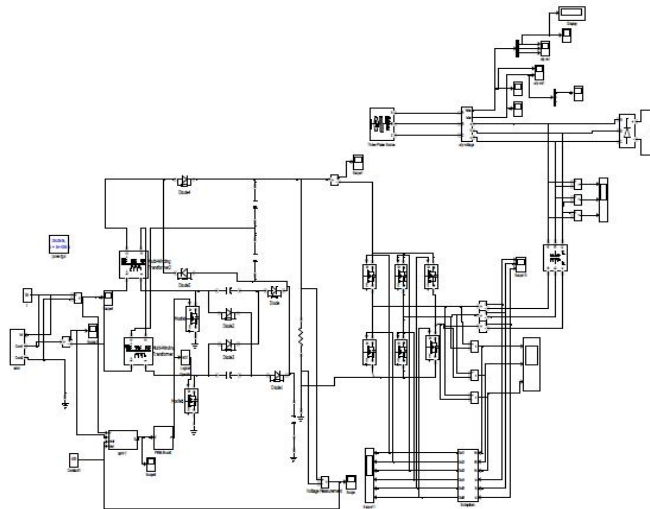


Fig.17. simulation circuit diagram of proposed system

Three Phase Grid Output Voltage Waveform:

The Fig.18 represents the waveform of the Three Phase Grid Output Voltage. In the below graph the X-axis represents the time period and Y-axis represents the amplitude of the Three Phase Grid Output Voltage. From the waveform we can observe the Grid Output Voltage range is 420V

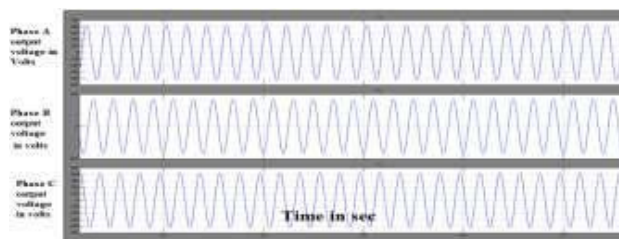


Fig.18. Grid output voltage waveform

Total Harmonic Distortion:

The Fig.19. represents the FFT analysis of the proposed system. In the below graph the X-axis represents the frequency and Y-axis represents the amplitude of the current. From the waveform we can observe the Total Harmonic Distortion range is 0.11%.

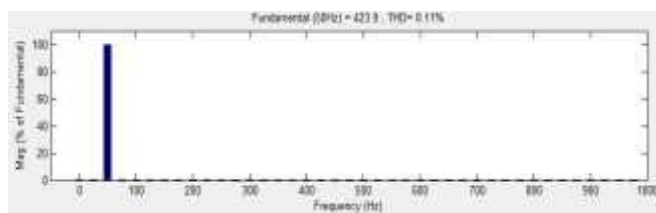


Fig.19. FFT analysis of proposed system

Comparison between the existing and proposed system

From the below comparison table we can easily identify that the relation between existing and proposed system. Based on that we can measure the reduced harmonic range is 89%. Thus the reduced total harmonic distortion range of proposed system is more efficient to uses in many applications.

TABLE.IV

Parameter of analysis	Existing system without high step up boost converter and with MPPT-PI controller	Proposed system with High step-up boost converter and MPPT-Fuzzy logic controller
Total Harmonic Distortion	1.26%	0.11%

VI. CONCLUSION

The simulations of double purpose, three-phase Solar Photovoltaic system have been carried out with power quality improvement in the AC distribution system. The performance of presented Solar Photovoltaic System along with harmonics compensation has been analysed and reduced. The advantages of ILST control algorithm have been found easy to implement, very fast convergence, and it requires only very less computational effort.

REFERENCES

- [1] Bhim Singh, Chinmay Jain and Sagar Goel "ILST Control Algorithm of Single-Stage Dual Purpose Grid Connected Solar PV System", IEEE Trans. Power Electronics, vol.29, no.10, Oct.2014.
- [2] Kuo-Ching Tseng and Chi-Chih Huang "High Step-Up-Efficiency Interleaved Converter with Voltage Multiplier Module for Renewable Energy System", IEEE Trans. Industrial Electronics, vol.61, no.3, March 2014.
- [3] W. Libo, Z. Zhengming and L. Jianzheng "A Single-Stage Three-Phase Grid-Connected Photovoltaic System With Modified MPPT Method and Reactive Power Compensation", IEEE Trans. Power Electronics, vol.22, no.4, Dec.2007.
- [4] Raghav Khanna, Qin hao Zhang, William E. Stanchina, Gregory F. Reed, and Zhi-Hong Mao "Maximum Power Point Tracking Using Model Reference Adaptive Control", IEEE Trans. Power Electronics, vol.29, no.3, .2014.
- [5] Francisco Paz and Martin Ordonez "Zero Oscillation and Irradiance Slope Tracking for Photovoltaic MPPT", IEEE Trans. Power Electronics, vol.61, no.11, 2014.
- [6] Bhim Singh, and Sabha Raj Arya "Adaptive Theory-Based Improved Linear Sinusoidal Tracer Control for DSTATCOM", IEEE Trans. Power Electronics, vol.28, no.8, August 2013.
- [7] Qian Zhang, Changsheng Hu, Lin Chen, Ahmadreza Amirahmadi, Nasser Kutkut, Z. John Shen, and Issa Batarseh "A Center Point Iteration MPPT Method with Application on the Frequency-Modulated LLC Micro inverter", IEEE Trans. Power Electronics, vol.29, no, 2014.
- [8] Mohammed A. Elgendy, Bashar Zahawi, and David J. Atkinson "Assessment of the Incremental Conductance Maximum Power Point Tracking Algorithm", IEEE Trans. Sustainable Energy, vol.4, no. Jan 2013.
- [9] Hoonki Kim, Sangjin Kim, Chan-Keun Kwon, Young-Jae Min, Chulwoo Kim, and Soo-Won Kim, Member "An Energy-Efficient Fast Maximum Power Point Tracking Circuit in an 800- μ W Photovoltaic Energy Harvester", IEEE Trans. Power Electronics, vol.28, no.6. 2013.
- [10] Steven L. Brunton, Clarence W. Rowley, Sanjeev R. Kulkarni, and Charles Clarkson "Maximum Power Point Tracking for Photovoltaic Optimization Using Ripple-Based Extremum Seeking Control", IEEE Trans. Power Electronics, vol.25, no.10, Oct 2010.
- [11] Fangrui Liu, Shanxu Duan, Fei Liu, Bangyin Liu, and Yong Kang "A Variable Step Size INC MPPT Method for PV Systems", IEEE Trans. Power Electronics, vol.55, no.7, July 2008.
- [12] Hairul Nissah Zainudin and Saad Mekhilef "Comparison Study of Maximum Power Point Tracker Techniques for PV Systems", Proceedings of the 14th International Middle East Power Systems Conference (MEPCON'10), Cairo University, Egypt, December 19-21, 2010, Paper ID 278.
- [13] A. Dolara, R. Faranda, and S. Leva "Energy Comparison of Seven MPPT Techniques for PV Systems", J. Electromagnetic Analysis & Applications, 3: 152-162 doi:10.4236/jemaa.2009.13024 Published Online September 2009.
- [14] Moacyr Aureliano Gomes de Brito, Luigi Galotto, Jr., Leonardo Poltronieri Sampaio, Guilherme de Azevedo e Melo, and Carlos Alberto Canesin "Evaluation of the Main MPPT Techniques for Photovoltaic Applications", IEEE Trans. Industrial Electron, vol.6, no.3, March 2013.
- [15] A.Pradeep Kumar Yadav, S.Thirumaliah and G.Haritha "Comparison of MPPT Algorithms for DC-DC Converters Based PV Systems", International Journal of Advanced Research in Electrical, Electronics and Instrumentation Engineering, vol.1, no. 1, July 2012. (ISSN: 2278 – 8875).

International Journal of Innovative Research in Science, Engineering and Technology

An ISO 3297: 2007 Certified Organization

Volume 4, Special Issue 5, April 2015

International Conference On Emerging Trends in Engineering and Technology (ICETET'15)

On 13th & 14th March 2015

Organized by

Pandian Saraswathi Yadav Engineering College, Arasanoor, Sivagangai, Tamilnadu, India

- [16] A.K.Verma, B.Singh, and D.T. Sahani “MPPT and Voltage Balancing Control with Sensing Only Inductor Current for Photovoltaic-Fed, Three-Level, Boost-Type Converters”, IEEE Trans. Power Electron, vol.29, no.1, Jan. 2014.
- [17] Hung-Chi Chen and Wen-Jan Lin, “Grid interfaced solar photo-voltaic power generating system with power quality improvements at AC mains”, presented at the IEEE 3rd Int. Conf. Sustainable Energy Technol., Kathmandu, and Nepal, Oct. 2012.
- [18] S. Wu Du and J. M. Su, “Analysis of an improved harmonic currents detection method based on LST”, in Proc. 2nd Int. Conf. Artif. Intell, Manage. Sci. Electron. Commerce, 2011, pp. 3755-3759.